

# Challenges to the industrial melt-processing of conductive plastics

Choong Gabriel Y.H.<sup>1, 2 a)</sup> De Focatiis Davide S.A.<sup>1</sup>, Lidgett Mark J.<sup>2</sup>, Thornton Matthew J.<sup>2</sup> and Clifford Mike J.<sup>1</sup>

<sup>1</sup>*Faculty of Engineering, University of Nottingham, Nottingham, NG7 2RD, UK*

<sup>2</sup>*Haydale Composites Solution, Loughborough, LE11 1QJ, UK*

<sup>a)</sup>Corresponding author: gabriel.choong@nottingham.ac.uk

**Abstract.** In this work, we investigate the relationship between the timescales available for polymer mobility during processing and post-processing and the electrical resistivity of melt-processed thermoplastics filled with carbon nanoparticles. Post-process annealing below the glass transition temperature was one avenue explored to uplift electrical conductivity. Detailed analysis of available literature on thermoplastics filled with either graphite nanoplatelets or carbon nanotubes, and of relevant processing data suggests that the required timescale for shaping process or post-processing to obtain conductive material needs to be sufficiently longer than that of the base polymer characteristic relaxation time  $\tau_d$ . Four factors have been identified that promote the formation of a conductive filler network in thermoplastics: filler loading content, polymer molar mass, processing temperature and processing timescales.

## INTRODUCTION

The preferred industrial processing route to incorporate graphite nanoplatelets (GNPs) or carbon nanotubes (CNTs) into thermoplastics is melt compounding. These compounds, made either by direct compounding or by masterbatch dilution, are subsequently formed into parts through further melt-processing. The bulk material properties, particularly the electrical properties, are strongly dependent on the nanocomposite morphology obtained in the melt and frozen-in by subsequent cooling to form a part. It is widely known that achieving satisfactory filler dispersion in melt-mixing is a major challenge. This is further complicated by the influence of filler geometry from various commercial carbon nanoparticle suppliers [1]. In addition, specific properties are associated with different filler network morphologies. For example, secondary agglomeration promotes electrical conductivity whereas good dispersion and distribution of the particles are required for mechanical property enhancement.

Despite these challenges, there is significant commercial interest in employing traditional melt processing equipment to produce GNP-filled thermoplastics with electrical conductivity uplifts due to both production cost and volume considerations. The two challenges faced in this work were: (1) rapid processing is unfavourable for electrical conductivity, and (2) certain parts may be unsuitable for long timescale melt processing due to factors such as intricate shapes and production cost.

Previous studies have focused on material-related (e.g. filler loading content and polymer type) and compounding equipment-related factors (e.g. extruder parameters) [2, 3]. Relaxation of the polymer is the dominant relaxation mechanism in nanocomposite rheology [4], and therefore here, we look at whether and how polymer mobility can be used to drive the re-organisation of the filler network as a post-processing procedure. Thermal annealing is one such method, and we explore this on injection moulded GNP filled amorphous thermoplastic as a possible route to enhance electrical conductivity. The focus of this work is to find a link between the timescales available for polymer mobility during processing, and the resulting electrical conductivity of processed parts. The aim is to identify a suitable route to develop carbon-filled conductive plastics by appropriate selection of both the materials and processes, with the goal of achieving savings in both cost and development time.

## MATERIAL AND METHODS

All polymer materials used in this work are commercial grade plastics. Acrylonitrile-butadiene-styrene (ABS) and polypropylene (PP) were both filled with 10 wt% of unfunctionalised GNP. The materials were compounded using a twin-screw extruder and pelletised in a commercial environment.

Injection moulding (IM) was performed to produce plate specimens with dimensions of 100 mm × 80 mm × 3.2 mm at a temperature of 235 °C in a commercial setting. Compression moulding (CM) using flash moulds [5] was employed to produce disc specimens at a temperature of 200 °C in two sizes: Ø 25 mm × 0.5 mm and Ø 65 mm × 2 mm.

Annealing parameters were identified through thermal and rheological characterisation. Rheometry of unfilled ABS was performed with an Anton Paar MCR 302 equipped with a torsional shear geometry. Measurements were carried out at a frequency range 100 – 0.1 rad s<sup>-1</sup> at 0.01% strain for a temperature  $T$  range of 100 – 135 °C. Isothermal frequency sweeps were shifted using an Arrhenius equation to determine the time-temperature dependence of unfilled ABS. The glass transition temperature  $T_g$  of ABS-GNP was determined as 138 °C using a Linkam DSC600 with a heating rate of 10 °C min<sup>-1</sup>. Annealing of IM plaque was performed at  $T = 130$  °C in a Memmert Universal oven; at this temperature, the relaxation time of unfilled ABS was  $\tau_d = 9.7 \times 10^3$  s.

Volume resistivity  $\rho$  was measured using a Keithley 8009 resistivity test fixture with a Keithley 6517B electrometer as the voltage source. Specimens were electrified with 100 V for 60 s in accordance to ASTM D257-14 [6]. After set annealing times, plaques were removed from the oven and quenched in a water bath, followed by thorough drying with paper towels prior to each electrical measurement.

Time-temperature dependences of the unfilled ABS and PP in the melt state were determined using rheometry. Isothermal frequency sweeps were performed using a Ø 25mm parallel plate geometry with a 0.5 mm gap size in an air atmosphere. Unfilled materials were measured between 250 °C and 140 °C. The frequency range was 100 – 0.1 rad s<sup>-1</sup> at 1% strain. Mastercurves were obtained by applying time-temperature superposition (considering horizontal shifting only) using a procedure detailed in [4]. The relaxation time  $\tau_d$  was determined from the inverse of the cross-over frequency of each mastercurve shifted to the desired reference  $T$ .

## RESULTS AND DISCUSSION

### Ratio of processing timescale to $\tau_d$

In order to assist on decision making for both matrix and processing timescales, we determined the ratio of the processing timescale  $t$  to  $\tau_d$  of the unfilled polymer; this is subsequently referred to as the relaxation time fraction,  $t / \tau_d$ , which is typically a number greater than unity in typical processes. The polymer melt undergoes a cooling profile during IM, and thus relaxes by a varying amount as  $\tau_d$  also changes with temperature. The average mould temperature  $\bar{T}$  is obtained from the Fourier series solution for 1-dimensional cooling of a plate, given by

$$\bar{T}(t) = T_e + (T_{\text{initial}} - T_e) \sum_{\text{odd } n} \frac{8}{n^2 \pi^2} \exp\left(-\frac{n^2 \pi^2 \alpha t}{4 L^2}\right)$$

where  $T_e$  = mould  $T$ ,  $T_{\text{initial}}$  = melt  $T$ ,  $\alpha$  = polymer thermal diffusivity,  $t$  = time, and  $2L$  = plate thickness.

The total relaxation time fraction for a given cooling profile is determined by numerically integrating  $\int dt / \tau_d$  over the cooling profile, and at each  $\bar{T}$ ,  $\tau_d$  was determined using Williams-Landel-Ferry (WLF) equation by shifting to the desired  $\bar{T}$ . The lower limit of  $\bar{T}$  was set to the material's  $T_g$ . The number of terms of the Fourier series solution  $n$  was fixed at 49 to improve the description of the high temperature profile in the initial cooling stage.

In the case of CM, we calculated  $t / \tau_d$  using only the isothermal holding period as this is dominant over the contributions of the heating and cooling periods. Fig. 1 shows a comparison of  $\rho$  as a function of the fractional relaxation time for the corresponding IM and CM melt-processes.

It is recognised that there are other factors that influence the electrical resistivity of an IM specimen, such as shear effects and filler orientation. However, it should be noted that the typical rapid processing timescales significantly limit the system's ability to rearrange the filler network to a state that favours electrical conductivity. Therefore, as a first approximation, the polymer's fractional relaxation time is used as an indicator of the feasibility of obtaining a conductive material.

## Thermal annealing

Evolution of volume resistivity as a function of the fractional relaxation time of GNP-filled ABS (10 wt%) for different moulding processes and including post-processing annealing is presented in Fig. 1. Here the fractional relaxation taking place during annealing is added to that during processing with the same method. After 22 hours of annealing at 130 °C,  $\rho$  of IM ABS-GNP decreased by an order of magnitude relative to the same material without annealing. By changing the timescale of the shaping process from IM to CM,  $\rho$  of the identical ABS-GNP material decreased by 9 orders of magnitude. This suggests that the annealing procedure resulted in limited additional polymer mobility to modify the filler network to create more conductive pathways.

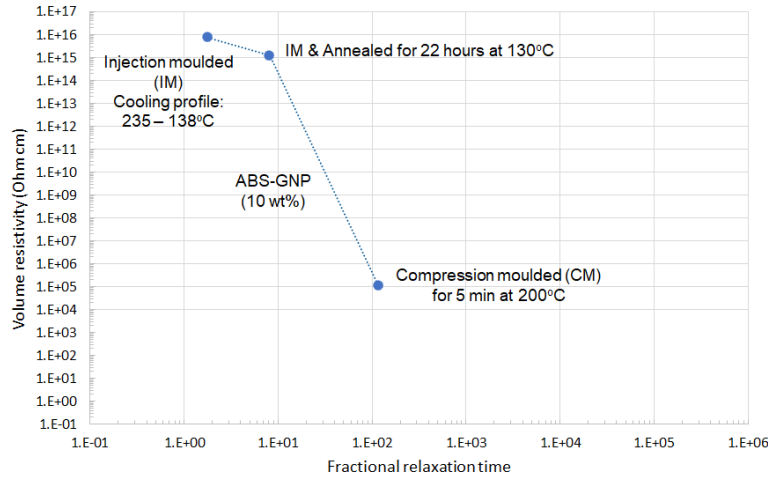
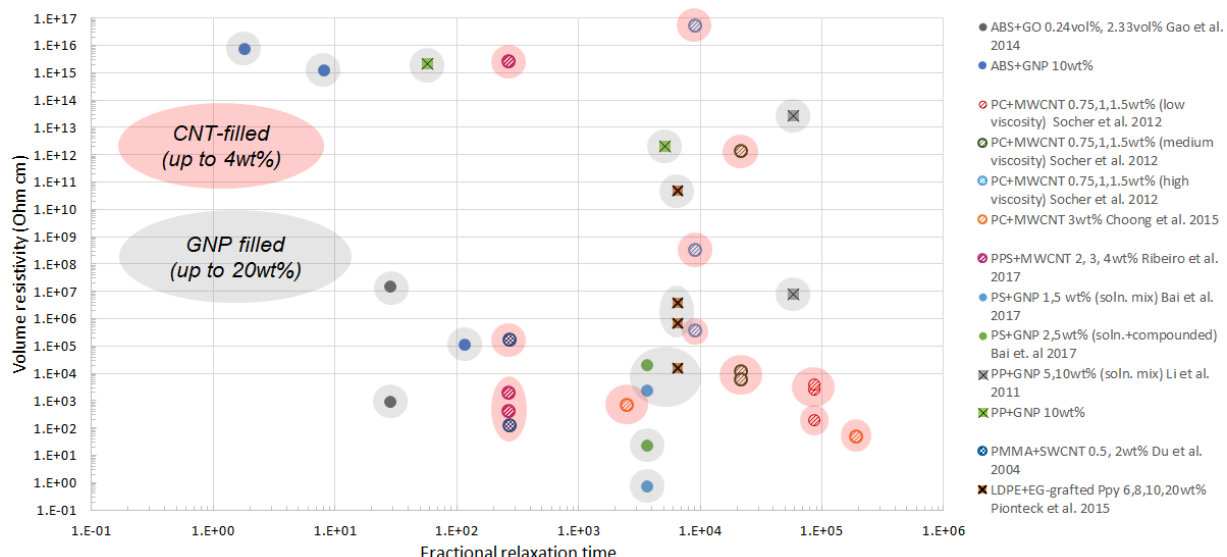


**FIGURE 1.** Electrical resistivity as a function of the fractional relaxation time of injection moulded, injection moulded and annealed, and compression moulded GNP-filled ABS (10 wt%). *Dotted lines are a guide to the eye*

## Thermoplastics filled with carbon nanoparticles

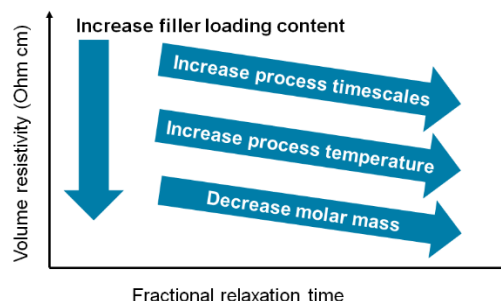
The technique described in the previous section was employed to analyse literature results. Literature [7-15] was selected based on the availability of three components of required information: (1) the rheological response from which to identify the time-temperature dependence of the unfilled matrix and  $\tau_d$ ; (2) sufficient specimen preparation parameters to obtain the temperature history (CM/IM); and (3) direct current volume resistivity measurements. In cases where the time-temperature dependence of the matrix was not directly available, it was obtained from published data on similar materials since this does not vary significantly between polymers of different grades [4].

Fig. 2 displays volume resistivity obtained from either GNP or CNT filled thermoplastics (semi-crystalline and amorphous) as a function of the fractional relaxation time on a wide range of literature studies. The plot suggests that it is easier to decrease  $\rho$  with CNTs at lower filler loading content; in addition, it can also be seen that, at least for the cases shown here, filled amorphous polymers also tend to achieve lower  $\rho$  when compared to filled crystalline materials.



**FIGURE 2.** Volume resistivity as a function of the fractional relaxation time (multiple) for two different types of carbon nanoparticle fillers

From the literature, we identified four factors that contribute to the reduction of  $\rho$ , as displayed in Fig. 3: (1) increasing the filler loading content, (2) increasing the process timescales, (3) increasing the processing temperature and (4) decreasing the polymer molar mass. Factors (3) and (4) are supported by Zeiler et al.'s findings that the CNT network formation is enhanced with higher temperature and lower molar mass [15]. It is plausible to consider that the same factors apply to GNP-filled thermoplastics, although there is limited experimental evidence in published literature of this at present. In addition, factors (2) and (3) are both exposed to the risk of polymer degradation that can be detrimental to the nanocomposite bulk properties. Long processing timescales and temperature can also be constrained by external factors such as manufacturing costs, making such processes commercially unattractive.



**FIGURE 3.** Material-related and process-related factors that promote electrically conductive filled thermoplastics

Fig. 4 illustrates the regions of interest for the development of conductive thermoplastics. There are 4 regions, labelled as: (1) Insulating, (2) Future target, (3) Likely viable commercially and (4) Not likely viable commercially. Region (1) is where the filled polymer systems have not yet reached the electrical percolation threshold. Region (2) includes conductive materials that can be processed rapidly – it is where one might aspire to be, but as yet has no reported results in the literature; Region (3) is where the bulk of the current conductive nanocomposite systems lie, depending on the conductivity, they are suitable for either electrostatic discharge or full electrical conductivity; Region (4) is similar to region (3) but timescales make these polymers less commercially viable due to long processing times and the risk of polymer degradation. Precise boundaries between the regions are somewhat arbitrary and should be tailored according to user requirements. Also, the diagram is not intended to identify materials that are commercially viable from the literature, but rather to aid the planning for the selection of both the material and the process that is most likely to be commercially relevant. It is worth mentioning that since Fig. 3 identifies the factors that influence  $\rho$ , it serves as an approximation tool and can provide a strategy to further decrease  $\rho$  when Fig. 4 is populated with the relevant data.

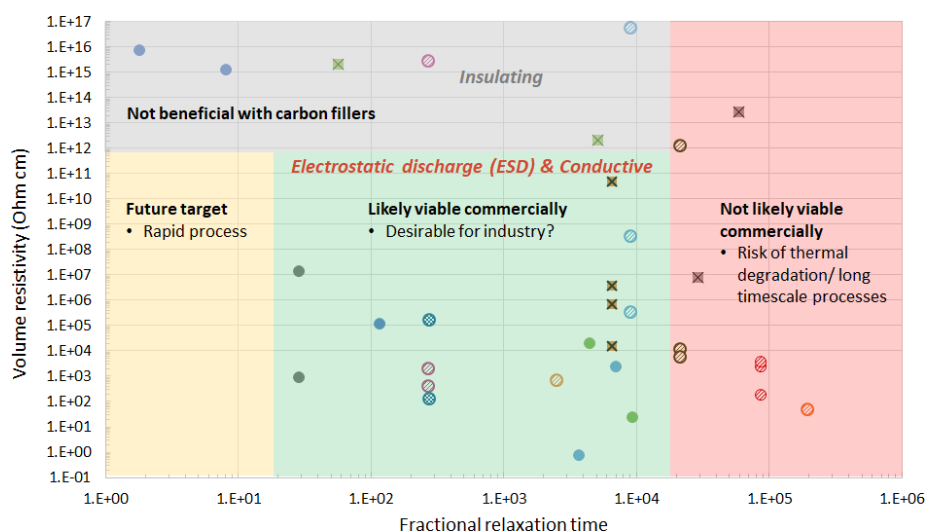


**FIGURE 4.** Volume resistivity of carbon nanoparticle-filled thermoplastics as a function of the fractional (multiple) relaxation time. The coloured segments indicate regions of interest to assist in both material and process selection when developing electrically conductive materials. *There is no intention to identify commercially viable materials from the literature*

## CONCLUSIONS

This work has shown that uplifts in electrical conductivity of carbon nanoparticle based thermoplastic can be achieved if the timescales of the shaping or post-processing are sufficiently greater than the matrix polymer's relaxation time  $\tau_d$ . In addition, four factors that promotes the formation of a conductive filler network in thermoplastics were identified from the literature: lower polymer molar mass, increased filler loading content, higher processing temperature, and longer process timescales.

## ACKNOWLEDGMENTS

The authors would like to acknowledge Innovate UK for part-funding this work through the Knowledge Transfer Partnership scheme (ref. KTP 010109).

## REFERENCES

1. Müller M.T., Hilarius K., Liebscher M., Lellinger D., Alig I., Pötschke P., *Materials*, **10**, 5, 545 (2017).
2. Khanam P.N., AlMaadeed M.A., Ouederni M., Harkin-Jones E., Mayoral B., Hamilton A., Sun D., *Vacuum*, **130**, 63–71 (2016).
3. Kalaitzidou K., Fukushima H., Askeland P., Drzal L.T., *J. Mater. Sci.*, **43**, 8, 2895 – 2907 (2008).
4. Choong G.Y.H., De Focatiis D.S.A., Hassell D.G., *Rheol. Acta*, **52**, 8-9, 801–814 (2013).
5. De Focatiis D.S.A., *Polym. Test.*, **31**, 4, 550–556 (2012).
6. ASTM, 'D257-14', Standard Test Methods for DC Resistance or Conductance of Insulating Materials (2014).
7. Gao C., Zhang S., Wang F., Wen B., Han C., Ding Y., Yang M., *ACS Appl. Mater. Interfaces*, **6**, 15, 12252–12260 (2014).
8. Socher R., Krause B., Muller M. T., Boldt R., Pötschke P., *Polym.*, **53**, 2, 495–504 (2012).
9. Choong G.Y.H., Lew C.Y., De Focatiis D.S.A., *J. Appl. Polym. Sci.*, **132**, 42277 (2015).
10. Ribeiro B., Pipes R.B., Costa M.L., Botelho E.C., *J. Comp. Mat.*, **51**, 2, 199–208 (2017).
11. Bai Q., Wei X., Yang J., Zhang N., Huang T., Wang Y., *Compos. Part A Appl. Sci. Manuf.*, **96**, 89–98 (2017).
12. Li Y., Zhu J., Wei S., Ryu J., Sun L., Guo Z., *Macromol. Chem. Phys.*, **212**, 18, 1951–1959 (2011).
13. Du F., Scogna R.C., Zhou W., Brand S., Fisher J.E., Wiley K.I., *Macromol.*, **37**, 24, 9048–9055 (2004).
14. Pionteck K., Valdez E.M.M, Piana F., Omastová M., Luyt A.S., Voit B., *J. Appl. Polym. Sci.*, **132**, 20 (2015).
15. Zeiler R., Handge U.A., Dijkstra D.J., Meyer H., Altstädt V., *Polym.*, **52**, 2, 430–442 (2010).